

KL-VS heterozygosity is associated with lower amyloid-dependent tau accumulation and memory impairment in Alzheimer's disease

Neitzel et al., Supplementary Information:

Supplementary Table 1 Main effect of global amyloid-PET levels on tau-PET levels

| Cross-sectional analysis | | |
|---|---|---|
| | KL-VS^{het} carriers, N144 | KL-VS^{het} non-carriers, N407 |
| Tau-PET SUVR, inferior temporal ROI | beta = 0.252, p = 0.002 | beta = 0.441, p = 2e-16 |
| Tau-PET SUVR, global ROI | beta = 0.279, p = 0.002 | beta = 0.433, p = 2e-16 |
| Longitudinal analysis | | |
| | KL-VS^{het} carriers, N52 | KL-VS^{het} non-carriers, N148 |
| Tau-PET annual change rate, inferior temporal ROI | beta = 0.183, p = 0.279 | beta = 0.391, p = 2.06e-06 |
| Tau-PET annual change rate, global ROI | beta = 0.142, p = 0.401 | beta = 0.275, p = 0.001 |

Supplementary Table 2 KL-VS^{het} × amyloid-PET interaction on regional tau-PET levels

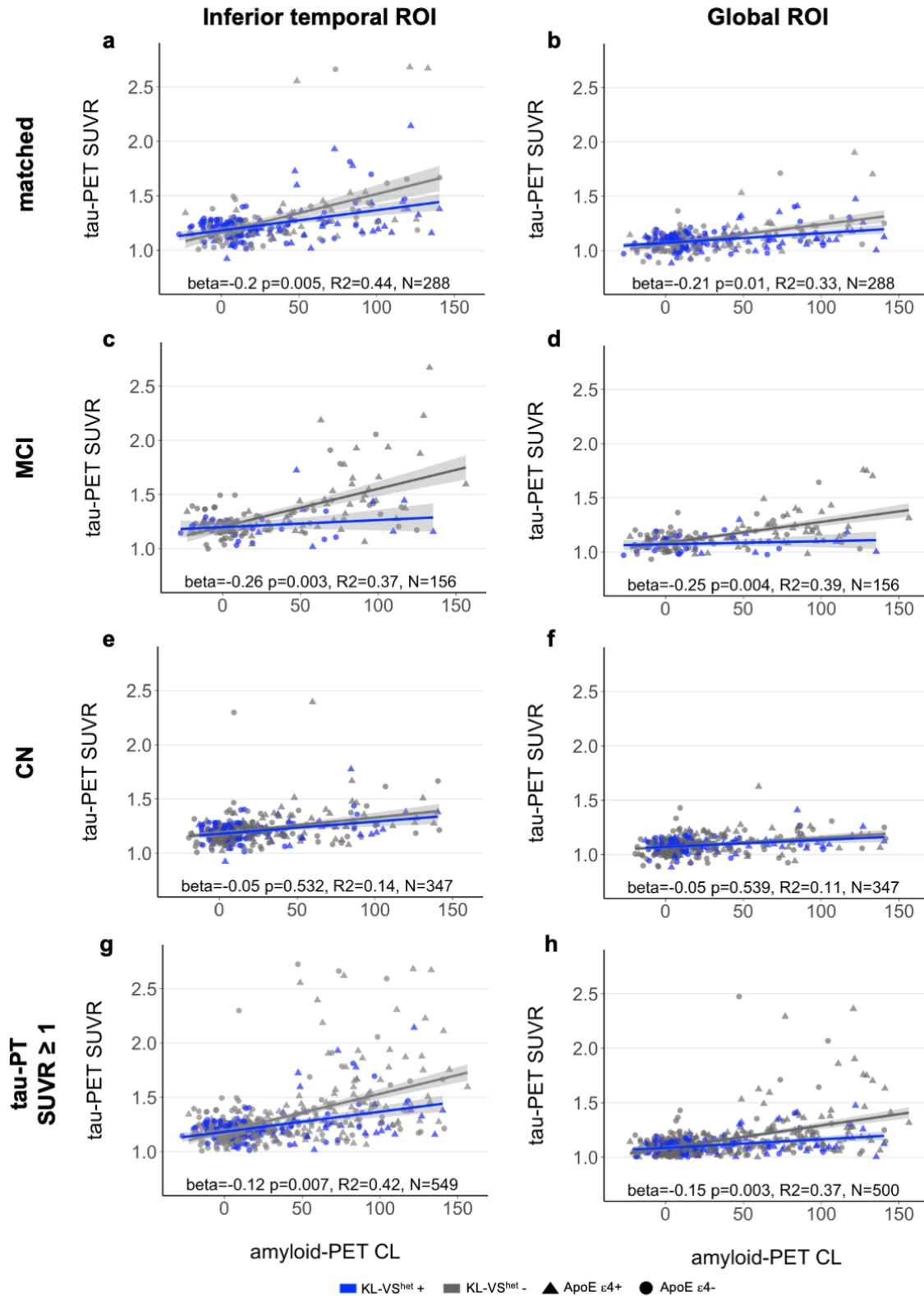
| Desikan-Kiliany region (left hemisphere) | Estimate | SE | T-value | P-value | P-value_[FDR-adj] |
|---|-----------------|-----------|----------------|----------------|------------------------------------|
| middletemporal | -0,0024 | 0,00052 | -4,6615 | 4,88E-06 | 0,00016 |
| inferiortemporal | -0,0023 | 0,00057 | -4,1290 | 4,82E-05 | 0,00055 |
| inferiorparietal | -0,0018 | 0,00053 | -3,3714 | 0,00085 | 0,00484 |
| temporalpole | -0,0017 | 0,00037 | -4,5183 | 9,23E-06 | 0,00016 |
| bankssts | -0,0016 | 0,00060 | -2,6568 | 0,00834 | 0,01790 |
| fusiform | -0,0016 | 0,00051 | -3,0636 | 0,00240 | 0,00907 |
| superiortemporal | -0,0013 | 0,00036 | -3,6237 | 0,00035 | 0,00293 |
| entorhinal | -0,0013 | 0,00045 | -2,7880 | 0,00567 | 0,01554 |
| parahippocampal | -0,0012 | 0,00037 | -3,2819 | 0,00116 | 0,00565 |
| rostralmiddlefrontal | -0,0012 | 0,00034 | -3,4223 | 0,00071 | 0,00484 |
| frontalpole | -0,0011 | 0,00035 | -3,1073 | 0,00208 | 0,00886 |
| caudalmiddlefrontal | -0,0011 | 0,00039 | -2,7723 | 0,00594 | 0,01554 |
| precuneus | -0,0010 | 0,00038 | -2,7141 | 0,00706 | 0,01715 |
| posteriorcingulate | -0,0010 | 0,00037 | -2,6325 | 0,00895 | 0,01790 |
| medialorbitofrontal | -0,0010 | 0,00032 | -2,9762 | 0,00318 | 0,00981 |
| parstriangularis | -0,0009 | 0,00031 | -2,9932 | 0,00301 | 0,00981 |
| lateralorbitofrontal | -0,0009 | 0,00036 | -2,6062 | 0,00965 | 0,01822 |
| superiorfrontal | -0,0008 | 0,00029 | -2,6497 | 0,00852 | 0,01790 |

Supplementary Table 3

| | ADNI tau-PET sample | | ADNI amyloid-PET sample | | p-value |
|-----------------------------|-------------------------------|-----------------------------------|-------------------------------|-----------------------------------|---------------------------|
| | KL-VS ^{het} carriers | KL-VS ^{het} non-carriers | KL-VS ^{het} carriers | KL-VS ^{het} non-carriers | |
| N | 144 | 407 | 283 | 784 | |
| Age | 71.29(6.61) | 71.39(6.72) | 72.22(6.78) | 72.10(7.38) | 0.221 |
| Sex, F:M | 76:68 | 206:201 | 128:123 | 380:404 | 0.745 |
| Diagnosis, CN:MCI:ADD | 102:34:8 | 245:122:40 | 133:120:30 | 331:343:110 | <0.001 ^{a,b,c,d} |
| Education, y | 16.20(2.50) | 16.65(2.51) | 16.17(2.55) | 16.40(2.57) | 0.070 |
| MMSE | 28.17(2.43) | 28.11(2.82) | 27.97(2.39) | 27.81(2.56) | 0.168 |
| ApoE ε4 status, neg:pos | 90:54 | 255:152 | 163:120 | 454:330 | 0.326 |
| Global amyloid-PET, CL | 28.85(37.94) | 32.28(40.30) | 36.99(42.53) | 38.96(43.63) | 0.010 ^c |
| Amyloid-PET status, neg:pos | 89:55 | 232:175 | 146:137 | 400:384 | 0.039 ^c |

Group comparisons were performed using ANOVA for continuous and Kruskal-Wallis test for categorical outcome variables. Italic letters reflect the following post-hoc, pair-wise comparisons (two-sided):

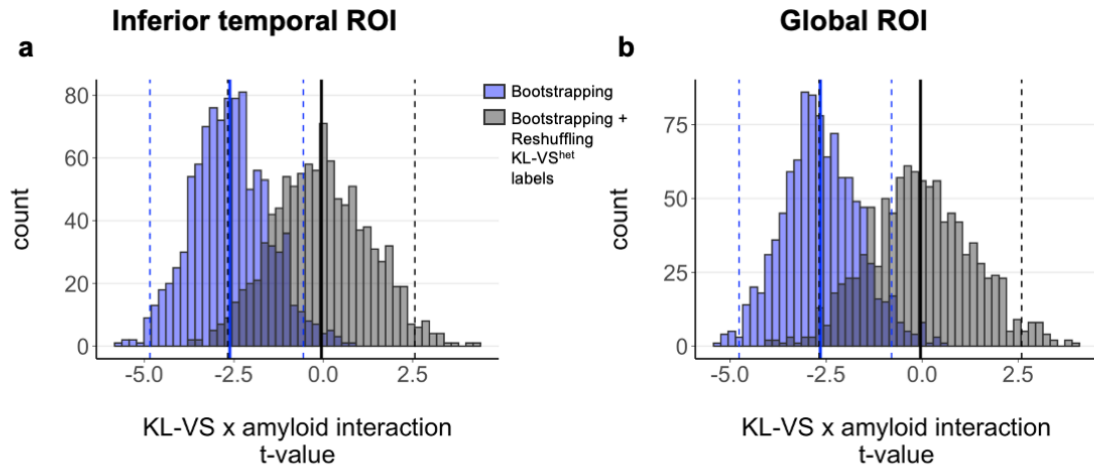
- ^a KL-VS^{het} carriers[tau-PET sample] versus KL-VS^{het} carriers[amyloid-PET sample],
^b KL-VS^{het} non-carriers[tau-PET sample] versus KL-VS^{het} non-carriers[amyloid-PET sample],
^c KL-VS^{het} carriers[tau-PET sample] versus KL-VS^{het} non-carriers[amyloid-PET sample],
^d KL-VS^{het} non-carriers[tau-PET sample] versus KL-VS^{het} carriers[amyloid-PET sample]



Supplementary Fig. 1 Association between KL-VS heterozygosity, amyloid- and tau-PET in different subsamples

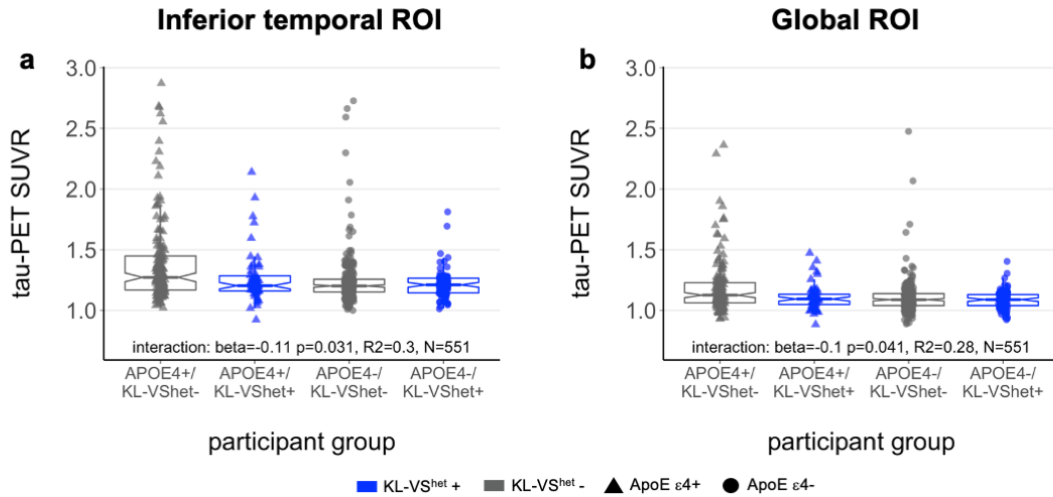
Scatterplots display the relationship between global amyloid-PET levels and tau-PET-levels measured in inferior temporal gyri (left panel) and globally in neocortical areas (right panel) as a function of KL-VS^{het} variant in **a, b** equally sized, matched KL-VS^{het} groups (144 KL-VS^{het}

carriers versus 144 non-carriers) according to propensity scores for diagnosis and global amyloid-PET levels, **c, d** only MCI patients, **e, f** only CN participants, and **g, h** only participants with tau-PET SUVR ≥ 1 . Blue and grey colour indicates individuals with heterozygous or non-heterozygous KL-VS^{het} alleles. Statistics of the KL-VS^{het} \times amyloid-PET interaction effect on tau-PET uptake were derived from multiple linear regression analyses, controlled for the main effects of KL-VS^{het} status and amyloid-PET levels as well as age, sex, education, ApoE $\epsilon 4$ carrier status and where applicable for diagnosis. Linear model fits are indicated together with 95% confidence intervals.



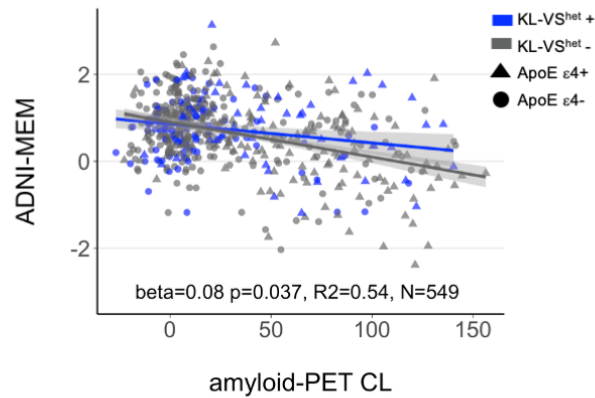
Supplementary Fig. 2 Association between KL-VS heterozygosity, amyloid- and tau-PET in 1,000 bootstrapped samples

Histograms display the distribution of the t-statistic estimating the $\text{KL-VS}^{\text{het}} \times \text{amyloid}$ interaction effect on tau-PET levels for the **a** inferior temporal ROI and **b** global ROI using 1,000 bootstrapping iterations (i.e. random sampling from the subject pool with replacement). The blue histograms show the bootstrapped results for the original data, while the grey histograms show the bootstrapped results for data in which the $\text{KL-VS}^{\text{het}}$ labels were randomly reshuffled on each iteration. Solid lines mark the mean and dashed lines the 95% confidence intervals of the respective t-statistic distributions.



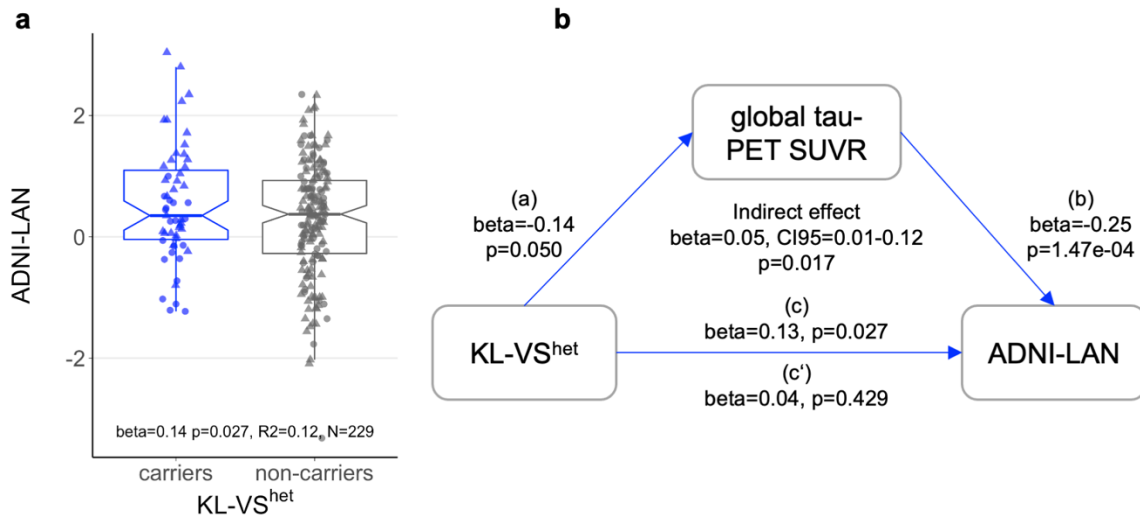
Supplementary Fig. 3 Association between KL-VS heterozygosity, ApoE $\epsilon 4$ carrier status and tau-PET levels

Boxplots show the relationship between tau-PET-levels measured in **a** inferior temporal gyri or **b** globally in neocortical areas as a function of KL-VS^{het} and ApoE $\epsilon 4$ carrier status. Blue and grey colour indicates individuals with heterozygous or non-heterozygous KL-VS alleles. Statistics of the KL-VS^{het} \times ApoE $\epsilon 4$ interaction effect on tau-PET uptake were derived from multiple linear regression analyses, controlled for the main effects of KL-VS^{het} and ApoE $\epsilon 4$ status as well as age, sex, education, diagnosis and lobal amyloid-PET levels. Boxplots show the 25th percentile, median, 75th percentile (box), 95% confidence intervals of the median (notch) and 1.5x IQR (whiskers).



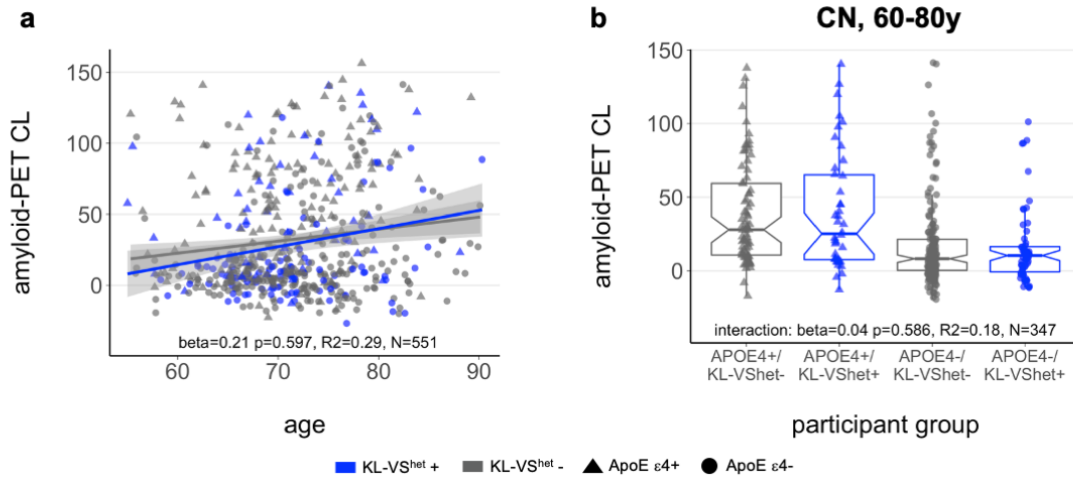
Supplementary Fig. 4 Association between KL-VS heterozygosity, amyloid-PET and memory

Scatterplots display the relationship between global amyloid-PET SUVR and memory functions dependent on KL-VS^{het} status. Blue and grey colour indicate individuals with heterozygous or non-heterozygous KL-VS alleles. Memory was measured based on an established composite score across different memory tests (ADNI-MEM). Statistical result of the KL-VS^{het} \times amyloid-PET interaction effect on memory was derived from multiple linear regression analysis, controlled for the main effects of KL-VS^{het} and amyloid-PET levels as well as age, sex, diagnosis, education and ApoE ϵ 4 carrier status. Two participants of the whole sample (N=551) had no ADNI-MEM scores. Linear model fits are indicated together with 95% confidence intervals.



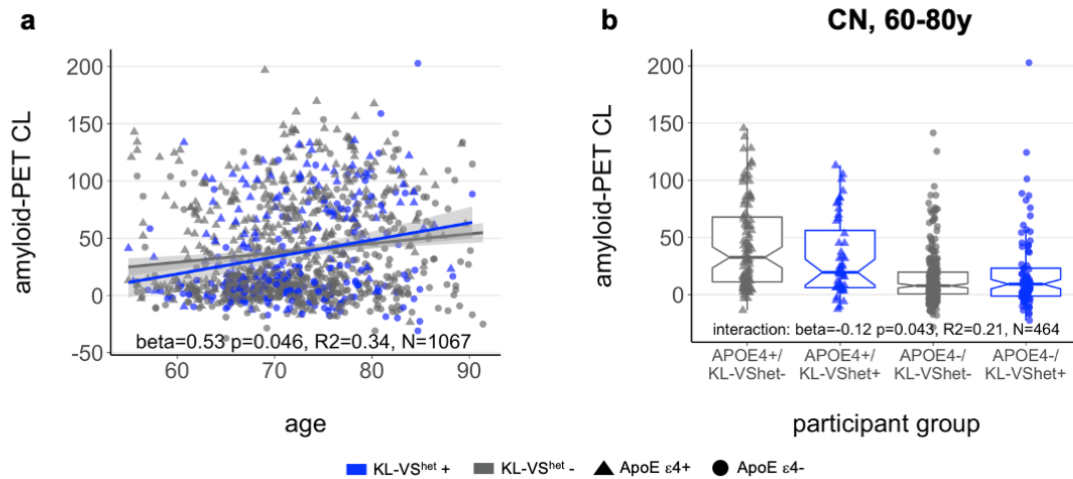
Supplementary Fig. 5 Lower tau-PET levels mediate beneficial effect of KL-VS heterozygosity on language performance in individuals with elevated amyloid-PET burden

a Boxplot shows language performance as a function of KL-VS^{het} variant in individuals with a positive amyloid-PET ($SUVR_{FBP} \geq 1.11$ or $SUVR_{FBB} \geq 1.08$). Blue and grey colour indicates individuals with heterozygous ($N = 55$) or non-heterozygous KL-VS alleles ($N = 174$). Language was measured by an established composite score, ADNI-LAN, based on test performance across multiple different language tests. Boxplots show the 25th percentile, median, 75th percentile (box), 95% confidence intervals of the median (notch) and 1.5x IQR (whiskers). **b** Path diagram of the mediation model showing that the association between KL-VS^{het} and better language performance is mediated via lower global tau-PET uptake. Path-weights are displayed as standardized beta values. All paths are controlled for age, sex, diagnosis, education, ApoE $\epsilon 4$ carrier status and continuous global amyloid-PET levels. Significance of the indirect effect was determined using bootstrapping with 10,000 iterations as implemented in the *mediation* package in *R*.



Supplementary Fig. 6 Association between KL-VS heterozygosity, age, ApoE ε4 carrier status and amyloid-PET levels

a The scatterplot displays the relationship between age and global amyloid-PET levels as a function of KL-VS^{het} status in the current ADNI sample (based on the availability of tau-PET assessment). Linear model fits are indicated together with 95% confidence intervals. **b** the boxplot displays global amyloid-PET levels as a function of KL-VS^{het} and ApoE ε4 status in a subgroup of cognitively unimpaired participants aged between 60 and 80 years, i.e. a subsample comparable to the one investigated in the original report on KL-VS^{het} effects on amyloid-PET¹³. Blue and grey colour indicates individuals with heterozygous or non-heterozygous KL-VS alleles. Statistics of the KL-VS^{het} × age or KL-VS^{het} × ApoE ε4 interaction effect on amyloid-PET uptake were derived from multiple linear regression analyses, controlled for the main effects of the interaction terms as well as sex, education, and where applicable diagnosis. Boxplots show the 25th percentile, median, 75th percentile (box), 95% confidence intervals of the median (notch) and 1.5x IQR (whiskers).



Supplementary Fig. 7 Confirmatory analyses in a larger sample: KL-VS heterozygosity effect on amyloid-PET levels

a The scatterplot displays the relationship between age and global amyloid-PET levels as a function of KL-VS^{het} status in all ADNI participants with amyloid-PET assessment (regardless of whether or not they underwent tau-PET assessment). Linear model fits are indicated together with 95% confidence intervals. **b** the boxplot displays global amyloid-PET levels as a function of KL-VS^{het} and ApoE ϵ 4 status in a subgroup of cognitively unimpaired participants aged between 60 and 80 years, i.e. a subsample comparable to the one investigated in the original report on KL-VS^{het} effects on amyloid-PET¹³. Note that we investigated the largest possible ADNI sample for this question in order to increase power and hence the likelihood to substantiate previously reported protective effects of KL-VS^{het} against amyloid accumulation. Blue and grey colour indicates individuals with heterozygous or non-heterozygous KL-VS alleles. Statistics of the KL-VS^{het} \times age or KL-VS^{het} \times ApoE ϵ 4 interaction effect on amyloid-PET uptake were derived from multiple linear regression analyses, controlled for the main effects of the interaction terms as well as sex, education, and where applicable diagnosis. Boxplots show the 25th percentile, median, 75th percentile (box), 95% confidence intervals of the median (notch) and 1.5x IQR (whiskers).